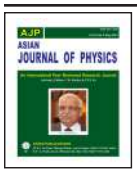

Asian Journal of Physics
Vol. 30, No 5 (2021) 00-00
Available on: www.asianjournalofphysics.in

ap

Coupled mode theory and coupled mode photonic devices: A Review

Enakshi Khular Sharma, Jyoti Prasad Nath and Nikhil Dhingra

Department of Electronic Science, University of Delhi South Campus

New Delhi-110 021, India

-Dedicated to Prof Anurag Sharma, FNA for his numerous contributions to Optics and Photonics.

A large number of guided wave photonic devices are based on coupling of guided modes between closely spaced waveguides or between guided modes of the same waveguide. Coupled mode analysis has been the most widely used method to study such coupling in which the interaction leads to transfer of power from one waveguide to the other or between modes of the same waveguide due to index perturbations. We present the coupled mode theory for evanescent field coupling between modes of two waveguides placed close to each other in context to the most versatile coupled mode device, a two-waveguide directional coupler. Its variants can be used to design a number of guided wave coupled photonic devices. We will illustrate by presenting a few such devices like switches and modulators, filters, polarizers and multiplexers for silicon photonic integrated circuits.

Keywords: Coupled mode theory, Coupled mode devices, Switches and Mode division multiplexers.

1 Introduction

Coupling of modes between waveguides or within guided modes of a waveguide has been an important study in fibre and integrated optics and is essential for the design of a large number of guided wave devices in contemporary photonic integrated circuits. Coupling is broadly of two types, the evanescent field coupling between modes of two adjacent waveguides or fibres and coupling between modes of the same fibre or waveguide due to periodic index perturbations. A large number of integrated optical devices such as directional couplers, power dividers, modulators, switches etc. consist of coupled waveguides in which the interaction of the evanescent tails of the guided modes of neighbouring waveguides leads to coupling of power from one waveguide to the other. Similarly, periodic gratings in optical fibres or waveguides like fibre Bragg gratings and long period gratings result in coupling between co-propagating or counter-propagating guided modes of the waveguide itself. Coupled Mode Theory [1-5] has been the most widely used analytical method for the study of coupled optical waveguides and waveguide modes. It is an analytical method which can be implemented for analysis of mode coupling in which the interaction of the evanescent tails of the guided modes of neighbouring waveguides leads to transfer of power from one waveguide to the other or when power is coupled between modes of the same waveguide due to index perturbations. In this article, we will discuss in detail coupled mode theory in context to the most successful and versatile coupled waveguide device, the directional coupler which works on evanescent field coupling between modes of two waveguides placed close to each other. Although in its simplest form it acts as a beam splitter, its variants can be designed to be used as more complicated devices such as switches and modulators, filters and polarizers.

Over the last decade, there has been growing interest in silicon-on-insulator (SOI) integrated optics because of its low loss in the telecommunication wavelength of 1550 nm and compatibility with the existing

Corresponding author
e mail: enakshi@south.du.ac.in (Enakshi Khular Sharma)

state-of-the-art CMOS fabrication technology. More recently, a complimentary platform of silicon nitride (Si_3N_4) photonics also compatible with the foundry-scale processes has emerged as an integration platform with low propagation losses over a wide wavelength range from 400 nm to 2350 nm. Hence, for all illustrative examples in our discussions on coupled mode analysis we have used silicon on insulator waveguides. We also present designs of some recently designed waveguide devices on the silicon-on-insulator and silicon nitride platforms based on interesting variants of the simple directional coupler.

2 Coupled mode theory

Figure 1 shows typical dielctric channel waveguides, specifically chosen as a silicon-on-insulator (SOI) waveguide with a silicon high index guiding layer (refractive index ~3.48) on a silica substrate (refractive index ~1.44) with an air/silica cover. The waveguides support propagating guided modes with specific electric and magnetic field configurations which are solutions of the Maxwell's equations with appropriate boundary conditions and propagate along the waveguide with only a phase change defined by the corresponding propagation constants.

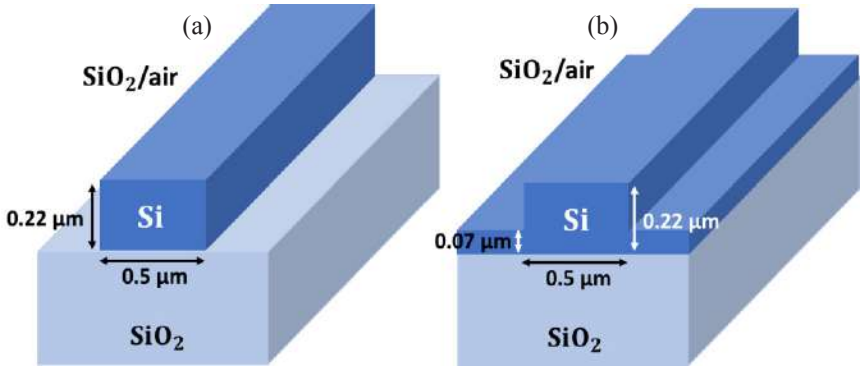

Fig 1. Typical silicon on silica insulator (SOI) (a) ridge or strip waveguide and (b) rib waveguide with silica or air /cover.

For waveguides with two-dimensional confinement, shown in Fig 1, analytical solutions are not always possible and numerical techniques such as Finite Element Method (FEM) or Finite Difference Method (FDM) need to be used to study the modes of the waveguides. All mode field calculations for two-dimensional waveguides here are based on FEM built in the FIMMWAVE solver of the Photon Design Software [6]. The modes supported are, in general, designated as quasi-TE and quasi-TM depending on their dominant field components. Figure 2 shows the variation of the electric and magnetic fields of the TE modes supported by such a single mode waveguide with thickness h = 220 nm and width w = 430 nm. The figures clearly show that the fields extend evanescently into the cover and substrate regions.

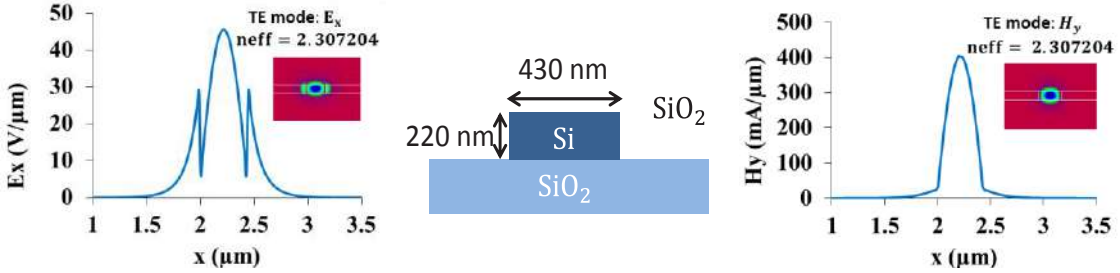

Fig 2. Modal profiles of the dominant fields, E_x and H_y, of the TE mode in a typical single moded silicon on silica strip waveguide with silica cover at λ = 1550 nm. Refractive indices of silicon and silica are taken as 3.47571 and 1.44402 at λ = 1550 nm.

When one or more such waveguides are placed in close proximity, as shown in Fig 3, they are coupled through their evanescent fields and power is exchanged between these waveguides as the guided modes propagate along these waveguides. The complete coupled waveguide geometry can be studied by obtaining a formal solution of the Maxwell's equations with boundary conditions to obtain the modes of the complete structure referred to as supermodes. However, Coupled Mode Theory (CMT) has been extensively used as a mathematical tool for analysis of wave propgation in coupled waveguides. Coupled Mode Theory is based on the assumption that the mode fields of individual waveguides do not change in the presence of the other waveguides and evolution of amplitudes of these modes in the coupled system is obtained as the solution of a set of coupled first order differential equations. This provides a clear and intuitive understanding of propagation and exchange of power among coupled waveguides. The solution also shows that the supermodes of the complete coupled system can be expressed as a linear combination of the individual waveguide modes. It may be mentioned that a modal analysis of the coupled waveguide configuration using a Variational Analysis with the trial field as a linear combination of the individual waveguide fields also yields the same results as coupled mode theory [7-9].

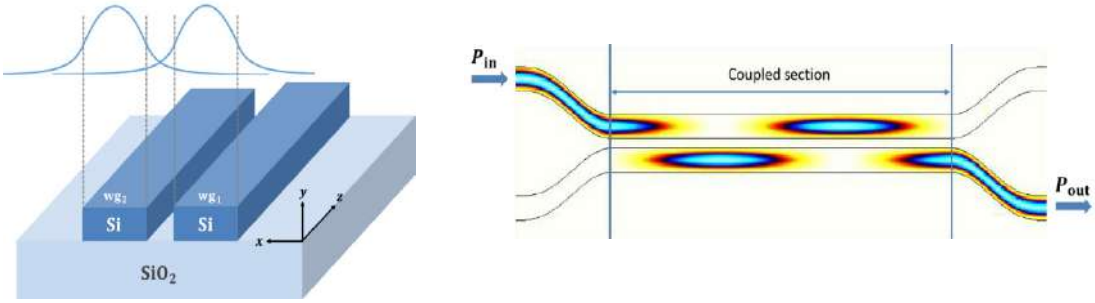

Fig 3. A typical configuration of two coupled silicon strip waveguides with top view of propagating intensity showing exchange of power due to evanescent coupling.

To resent the coupled mode analysis we consider the coupled waveguide configuration as shown in Fig 3. It is assumed that the guided total field in the coupled structure can be represented as the sum of the individual waveguide modes (each waveguide assumed to be single moded). Hence, we can write

$$\vec{E}(x, y, z) = A(z)\,\vec{E}_1(x, y)e^{-j\beta_1 z} + B(z)\,\vec{E}_2(x, y)e^{-j\beta_2 z}$$

$$\vec{H}(x, y, z) = A(z)\,\vec{H}_1(x, y)e^{-j\beta_1 z} + B(z)\,\vec{H}_2(x, y)e^{-j\beta_2 z} \quad (1)$$

where $A(z)$ and $B(z)$ represent the amplitudes of the propagating mode in waveguide1 (WG_1) and waveguide2 (WG_2), respectively. $\vec{E}_1(x, y)$, $\vec{H}_1(x, y)$ and $\vec{E}_2(x,y)$, $\vec{H}_2(x,y)$ are the transverse mode field profiles of the individual waveguides, which are assumed not to change in the presence of the second waveguide, and β_1 and β_2 are the corresponding propagation constants. The propagation constants are often expressed in terms of an effective index n_{eff} as $\beta = k_0\, n_{\text{eff}}$, where $k_0 = 2\pi/\lambda$. All the fields satisfy the Maxwell's equations

$$\vec{\nabla} \times \vec{E} = -j\omega\mu_0 \vec{H} \text{ and } \vec{\nabla} \times \vec{H} = j\omega\varepsilon_0 n^2 \vec{E} \quad (2)$$

Substituting the field of Eq (1) into the above Maxwell's equations one obtains,

$$(\hat{z} \times \vec{E}_1)\frac{dA}{dz} + (\hat{z} \times \vec{E}_2)\frac{dB}{dz} = 0 \quad (3)$$

$$(\hat{z} \times \vec{H}_1)\frac{dB}{dz} - j\omega\varepsilon_0 (n^2 - n_1^2)\,A\vec{E} + (\hat{z} \times \vec{H}_2)\frac{dB}{dz} - j\omega\varepsilon_0 (n^2 - n_1^2)\,B\vec{E}_2 = 0 \quad (4)$$

where $n^2(x, y)$ is the transverse refractive index profile of the coupled waveguide configuration, while $n_1^2(x, y)$

and $n_2^2(x, y)$ are the refractive index profiles of WG_1 and WG_2, respectively. Following the analysis given by Rumpf [10], we substitute the above equations into the following equations

$$\int_{-\infty}^{\infty}\int_{-\infty}^{\infty}[\vec{H}_1 \bullet (\text{Eq. 3}) - \vec{E}_1 \bullet (\text{Eq. 4})]\, dx\, dy = 0 \tag{5}$$

$$\int_{-\infty}^{\infty}\int_{-\infty}^{\infty}[\vec{H}_2 \bullet (\text{Eq. 4}) - \vec{E}_2 \bullet (\text{Eq. 5})]\, dx\, dy = 0 \tag{6}$$

After some algebraic manipulations the following coupled equations for the amplitudes $A(z)$ and $B(z)$ are obtained;

$$\frac{dA}{dz} + e_{12}\frac{dB}{dz}e^{-j(\beta_2-\beta_1)z} + jk_{11}A + jk_{12}B\,e^{-j(\beta_2-\beta_1)z} = 0 \tag{7}$$

$$\frac{dB}{dz} + e_{12}\frac{dA}{dz}e^{+j(\beta_2-\beta_1)z} + jk_{22}B + jk_{21}B\,e^{+j(\beta_2-\beta_1)z} = 0 \tag{8}$$

where κ_{pq} and e_{pq} ($p, q = 1$ or 2) are defined as,

$$\kappa_{pq} = \frac{\omega\varepsilon_0\int_{-\infty}^{\infty}\int_{-\infty}^{\infty}[n^2(x, y) - n_q^2(x, y)]\,\vec{E}_p(x, y) \bullet \vec{E}_q(x, y)\, dxdy}{2\int_{-\infty}^{\infty}\int_{-\infty}^{\infty}\hat{z} \bullet [\vec{E}_p(x, y) \times \vec{H}_p(x, y)\, dxdy} \tag{9}$$

$$e_{pq} = \frac{\int_{-\infty}^{\infty}\int_{-\infty}^{\infty}\hat{z} \bullet [\vec{E}_p(x, y) \times \vec{H}_q(x, y) + \vec{E}_q(x, y) \times \vec{H}_p(x, y)\, dxdy}{2\int_{-\infty}^{\infty}\int_{-\infty}^{\infty}\hat{z} \bullet [\vec{E}_p(x, y) \times \vec{H}_p(x, y)\, dxdy} \tag{10}$$

The terms e_{12} and e_{21} are an overlap of the fields of the two waveguides and define the excitation coefficients of the mode of one waveguide by the mode of the other waveguide and e_{11} and e_{22} are unity. If the waveguides are sufficiently apart, $e_{12} = e_{21} \approx 0$ and these terms are neglected in conventional coupled mode analysis. The terms κ_{12} and κ_{21} are the coupling coefficients which define the coupling between the waveguides, while κ_{11} and κ_{22} give the small perturbation correction to the propagation constants of the modes of the individual waveguides due to the presence of the other waveguide. If the waveguides are sufficiently apart, very often, in coupled mode analysis these terms are also neglected. The denominator in all the expressions is related to the normalization factor of the orthogonal modes of the waveguides. If the mode fields are normalized such that the power carried by the mode is 1 Watt, then

$$\int\int_{-\infty}^{\infty}\hat{z} \cdot [E_p(x, y) \times H_p^*(x, y)]dxdy = 1\text{W} \tag{11}$$

and the factor in the denominator is 2.

Alternatively, the corrections to the propagation constants κ_{11} and κ_{22} can be included in defining the propagation constants of the mode fields $\vec{E}_1$ and $\vec{E}_2$ in Eqs (1) as;

$$\begin{aligned}\vec{E}(x, y, z) &= A(z)\,\vec{E}_1(x, y)\,e^{-j\vec{\beta}_1 z} + B(z)\,\vec{E}_2(x, y)e^{-j\vec{\beta}_2 z}\\ \vec{H}(x, y, z) &= A(z)\,\vec{H}_1(x, y)e^{-j\vec{\beta}_1 z} + B(z)\,\vec{H}_2(x, y)e^{-j\vec{\beta}_2 z}\end{aligned} \tag{12}$$

where the corrected propagation constants are given by $\vec{\beta}_1 = \beta_1 + \kappa_{11}$ and $\vec{\beta}_2 = \beta_2 + \kappa_{22}$. Doing so and neglecting the overlap integrals e_{12} and e_{21}, the coupled Eqs (7) and (8) reduce to the following simple forms

$$\frac{dA}{dz} = -j\kappa_{12} B e^{-j(\vec{\beta}_2 - \vec{\beta}_1)z}$$
$$\frac{dB}{dz} = -j\kappa_{21} B e^{+j(\vec{\beta}_2 - \vec{\beta}_1)z} \tag{13}$$

The above equations can be combined to form the following uncoupled second order differential equation for $A(z)$,

$$\frac{d^2A}{dz^2} - j\Delta\beta \frac{dA}{dz} + \kappa^2 A = 0 \tag{14}$$

where $\kappa^2 = \kappa_{12} \times \kappa_{21}$ and $\Delta\beta = \vec{\beta}_2 - \vec{\beta}_1$. For synchronised waveguides with $\Delta\beta = 0$ or in the approximation that $e_{12} = e_{21} \approx 0$, it can be shown that $\kappa_{12} = \kappa_{21} = \kappa$ and the general solution for $A(z)$ and $B(z)$ are obtained as

$$A(z) = e^{i(\Delta\beta/2)z} [a_1 e^{-j\gamma z} + a_2 e^{+j\gamma z}]$$
$$B(z) = \frac{1}{\kappa} e^{i(\Delta\beta/2)z} \left[\left(\frac{\Delta\beta}{2} + \gamma \right) a_1 e^{-j\gamma z} + \left(\frac{\Delta\beta}{2} - \gamma \right) a_2 e^{+j\gamma z} \right] \tag{15}$$

where,

$$\gamma = \sqrt{\left(\frac{\Delta\beta}{2} \right)^2 + \kappa^2}$$

By use of the initial conditions, $A(0) = A_0$ and $B(0) = B_0$, , one can obtain the two constants a_1 and a_2 and hence the evolution of the mode amplitudes $A(z)$ in WG_1 and $B(z)$ in WG_2 are obtained as

$$A(z) = \left[\cos(\gamma z) + j \frac{\Delta\beta}{2\gamma} \sin(\gamma z) \right] A_0 - j \frac{\kappa}{\gamma} \sin(\gamma z) B_0$$
$$B(z) = -j \frac{\kappa}{\gamma} \sin(\gamma z) A_0 + \left[\cos(\gamma z) + j \frac{\Delta\beta}{2\gamma} \sin(\gamma z) \right] B_0 \tag{16}$$

which can be written as a transfer matrix given by

$$\begin{bmatrix} A(z) \\ B(z) \end{bmatrix} = \begin{bmatrix} \cos(\gamma z) + j \frac{\Delta\beta}{2\gamma} \sin(\gamma z) & -j \frac{\kappa}{\gamma} \sin(\gamma z) \\ -j \frac{\kappa}{\gamma} \sin(\gamma z) & \cos(\gamma z) + j \frac{\Delta\beta}{2\gamma} \sin(\gamma z) \end{bmatrix} \begin{bmatrix} A_0 \\ B_0 \end{bmatrix} \tag{17}$$

For synchronous waveguides (or phase matched waveguides) with $\Delta\beta = 0$, this reduces to

$$\begin{bmatrix} A(z) \\ B(z) \end{bmatrix} = \begin{bmatrix} \cos(\kappa z) & -j \sin(\kappa z) \\ -j \sin(\kappa z) & \cos(\kappa z) \end{bmatrix} \begin{bmatrix} A_0 \\ B_0 \end{bmatrix}$$

The powers carried by the modes propagating in the individual waveguides, WG_1 and WG_2 are given by $P_1 = |A(z)|^2$ and $P_2 = |B(z)|^2$, respectively. If initially power is launched only in WG_1, i.e. $B_0 = 0$, the evolution of amplitudes in the two waveguides is given by

$$A(z) = \left[\cos(\gamma z) + j \frac{\Delta\beta}{2\gamma} \sin(\gamma z) \right] A_0 \qquad B(z) = -j \frac{\kappa}{\gamma} \sin(\gamma z) A_0 \tag{18}$$

and power in the two waveguides is given by

$$P_2(z) = \frac{P_0}{1 + \left(\frac{(\Delta\beta)^2}{4\kappa^2} \right)} \sin^2(\gamma z) \text{ and } P_1(z) = P_0 - P_2 \tag{19}$$

where P_0 is the power initially launched in WG_1. Hence, there is a periodic exchange of power between the two waveguides with maximum power transfer occurring at the coupling length defined by $L_c = \pi/2\gamma$. It may

be noted that, at the coupling length, $z = L_c$, in non-synchronous waveguides (with $\Delta\beta \neq 0$) the power transfer to WG_2 is not complete; however, at $z = 2\,L_c$ the power returns completely to WG_1. For synchronous or phase matched waveguides (with $\Delta\beta = 0$), Eq (19) reduces to

$$P_2(z) = P_0 \sin^2(\kappa z) \text{ and } P_1(z) = P_0 \cos^2(\kappa z) \tag{20}$$

showing that complete power is transferred to WG_2 at $z = L_c = \pi/2\kappa$ and returns to at $z = 2L_c$, implying that it is possible to have a complete exchange of power between the waveguides. Also, for synchronous waveguides at an interaction length of $z = L_c/2$ one obtains a 3dB coupler in which the power is equally divided between the two waveguides, with an additional phase factor of $(-j)$ or $(-\pi/2)$ in the modal field of WG_2. It may be noted that at twice the coupling length the power returns to WG_1 with an additional phase factor of π in the amplitude.

3 Supermodes and coupled mode theory

As mentioned earlier, one can use Maxwell's equations to obtain the electromagnetic modes, referred to as supermodes, of the complete coupled waveguides configuration to study propagation. These supermodes can also be obtained in terms of the modes of the individual waveguides by the coupled mode analysis by solving the coupled mode amplitude Eqs (13) as follows: we redefine new variables a(z) and b(z) as

$$a(z) = A(z)\, e^{-j\vec{\beta}_1 z} \quad \text{and} \quad b(z) = B(z)\, e^{-j\vec{\beta}_2 z} \tag{21}$$

Equation (12) can be re-written as

$$\vec{E}(x, y, z) = a(z)\, \vec{E}_1(x, y) + b(z)\, \vec{E}_2(x, y)$$
$$\vec{H}(x, y, z) = a(z)\, \vec{H}_1(x, y) + b(z)\, \vec{H}_2(x, y) \tag{22}$$

and the coupled equations for $a(z)$ and $b(z)$ are obtained from Eqs (13) as

$$\frac{da}{dz} = -j\bar{\beta}_1 a - j\kappa b$$
$$\frac{db}{dz} = -j\bar{\beta}_2 b - j\kappa a \tag{23}$$

These can be combined to form the following second order differential equation for $a(z)$

$$\frac{d^2a}{dz^2} + j(\bar{\beta}_1 + \bar{\beta}_2)\frac{da}{dz} - (\bar{\beta}_1\bar{\beta}_2 - \kappa^2)a \tag{24}$$

which leads to two solutions of the form

$$a(z) = a_s\, e^{-j\beta_s z} \quad \text{and } a(z) = a_a\, e^{-j\beta_a z} \tag{25}$$

where, β_s and β_a are given by

$$\beta_{s,a} = \frac{\bar{\beta}_1 + \bar{\beta}_2}{2} \pm \sqrt{\left(\frac{\Delta\beta}{2}\right)^2 + \kappa^2} = \frac{\bar{\beta}_1 + \bar{\beta}_2}{2} \pm \gamma \tag{26}$$

and corresponding $a(z)$ and $b(z)$ are given by

$$b(z) = a_s \left(\frac{\Delta\beta}{2\kappa} + \frac{\gamma}{\kappa}\right) e^{-j\beta_s z} \text{ and } a(z) = a_a \left(\frac{\Delta\beta}{2\kappa} - \frac{\gamma}{\kappa}\right)\, e^{-j\beta_a z}$$

This implies that the coupled waveguide configuration supports two 'supermodes' with the modal fields given by

$$\vec{E}_s(x, y, z) = a_s[\vec{E}_1(x, y) + (b_s/a_s)\, \vec{E}_2(x, y)]\, e^{-j\beta_s z} \text{ and } \vec{E}_a(x, y, z) = a_s[\vec{E}_1(x, y) + (b_a/a_a)\, \vec{E}_2(x, y)]\, e^{-j\beta_s z}$$
$$\vec{H}_s(x, y, z) = a_s[\vec{H}_1(x, y) + (b_s/a_s)\, \vec{H}_2(x, y)]\, e^{-j\beta_s z} \text{ and } \vec{H}_a(x, y, z) = a_s[\vec{H}_1(x, y) + (b_a/a_a)\, \vec{H}_2(x, y)]\, e^{-j\beta_a z} \tag{27}$$

where $\frac{b_s}{a_s} = \left(\frac{\Delta\beta}{2\kappa} + \frac{\gamma}{\kappa}\right)$ and $\frac{b_a}{a_a} = \left(\frac{\Delta\beta}{2\kappa} - \frac{\gamma}{\kappa}\right)$. Hence, the modal field profiles of the supermodes of the total coupled configuration can be expressed in terms of the modal fields of the individual waveguides. The constants a_s and a_a are determined by the normalization.

Note that the difference in the propagation constants of the two supermodes, $\beta_s - \beta_a = \sqrt{\left(\frac{\Delta\beta}{2}\right)^2 + \kappa^2}$ will be minimum, when $\Delta\beta = 0$, or when the two waveguides are synchronous or phase-matched. This criterion is used to design phase matched waveguides in design of photonic devices based on coupled waveguides since the individual waveguide propagation constants $\bar{\beta}_2$ and $\bar{\beta}_1$ are perturbed by the presence of the other waveguide. It may also be noted that, for large values of $\Delta\beta$, it is possible to write $\frac{\gamma}{\kappa} = \sqrt{1 + \left(\frac{\Delta\beta}{2\kappa}\right)^2} \approx \left(\frac{\Delta\beta}{2\kappa}\right)$ and hence, the transverse mode profile for $\vec{E}_s(x, y)$ is dominantly $\vec{E}_2(x, y)$ while for $\vec{E}_a(x, y)$ it is $\vec{E}_1(x, y)$; note that we have considered $\beta_2 > \beta_1$.

If the two waveguides are identical or synchronous, i.e., with $\Delta\beta = 0$, it can be seen, $b_s = a_s$ and $b_a = -a_a$; that the two normalised supermodes can be written as,

$$\vec{E}_s(x, y, z) = \frac{1}{\sqrt{2}}[\vec{E}_1(x, y) + \vec{E}_2(x, y)]\, e^{-j\beta_s z} \quad \vec{E}_a(x, y, z) = \frac{1}{\sqrt{2}}[\vec{E}_1(x, y) - \vec{E}_2(x, y)]\, e^{-j\beta_s z}$$

$$\vec{H}_s(x, y, z) = \frac{1}{\sqrt{2}}[\vec{H}_1(x, y) + \vec{H}_2(x, y)]\, e^{-j\beta_s z} \quad \vec{H}_a(x, y, z) = \frac{1}{\sqrt{2}}[\vec{H}_1(x, y) - \vec{H}_2(x, y)]\, e^{-j\beta_a z} \tag{28}$$

with the propagation constants given by $\beta_s = \beta_0 + \kappa$ and $\beta_a = \beta_0 - \kappa$. Hence, for phase matched waveguides, the modal field of the "symmetric supermode" is the sum of the mode profiles of the individual waveguides while for the "antisymmetric mode" it is the difference. It may be mentioned that although the subscripts '*s*' and '*a*' are used in general for the supermodes, the modal profiles are symmetric and antisymmetric only when the waveguides are identical.

If power is launched into the phase matched coupled waveguide configuration by the modal field of WG_1, then at $z = 0$ one can write

$$\vec{E}_1(x, y) = c_s \vec{E}_s(x, y, 0) + c_a \vec{E}_a(x, y, 0) = c_s \frac{1}{\sqrt{2}}[\vec{E}_1(x, y) + \vec{E}_2(x, y)] + c_a \frac{1}{\sqrt{2}}[\vec{E}_1(x, y) + \vec{E}_2(x, y)] \tag{29}$$

where c_s and c_a are the excitation coefficients of the symmetric and antisymmetric mode. A simple comparison shows that $c_s = c_a = (\sqrt{2})^{-1}$ or the "symmetric" and "antisymmetric modes" are equally excited and each carries half the power or 0.5 P_0.

If one of the waveguides (WG_2) supports more than one mode as in a configuration often used for mode division multiplexing by evanescent coupling from a single mode waveguide, the total field of the coupled configuration can be written as

$$\vec{E}(x, y, z) = A(z)\, \vec{E}_1(x, y)\, e^{-j\bar{\beta}_1 z} + \sum_n B_n(z)\, \vec{E}_{2n}(x, y)\, e^{-j\bar{\beta}_{2n} z}$$

$$\vec{H}(x, y, z) = A(z)\, \vec{H}_1(x, y)\, e^{-j\bar{\beta}_1 z} + \sum_n B_n(z)\, \vec{H}_{2n}(x, y)\, e^{-j\bar{\beta}_{2n} z} \tag{30}$$

However, it can be shown that if the propagation constants of the multimode waveguide (WG_2) are well spaced, there is an interaction or exchange of power with only the specific mode which is phase matched to the mode in WG_1. The evolution of power in such a coupled system can also be studied by use of the two-mode coupled mode theory developed above by use of only the phase matched mode for the second waveguide.

4 Numerical simulations for two evanescently coupled waveguides

As mentioned earlier, the most successful and versatile coupled waveguide device is a directional coupler which makes use of evanescent field coupling between modes of two waveguides placed close to each other. In this section, we present results of some numerical simulations for two coupled waveguides which validate the various salient features obtained by coupled mode theory. We consider the typical directional coupler configurations formed with silicon on silica waveguides with silica cover. Figure 4 shows an identical waveguide directional coupler configuration formed by two silicon strip waveguides with a separation S. For a typical separation S = 250 nm, the exchange of power between the waveguides is shown when power is launched in WG_1. As predicted by the coupled mode analysis there is a periodic exchange of power between the waveguides with complete power transfer at the coupling length.

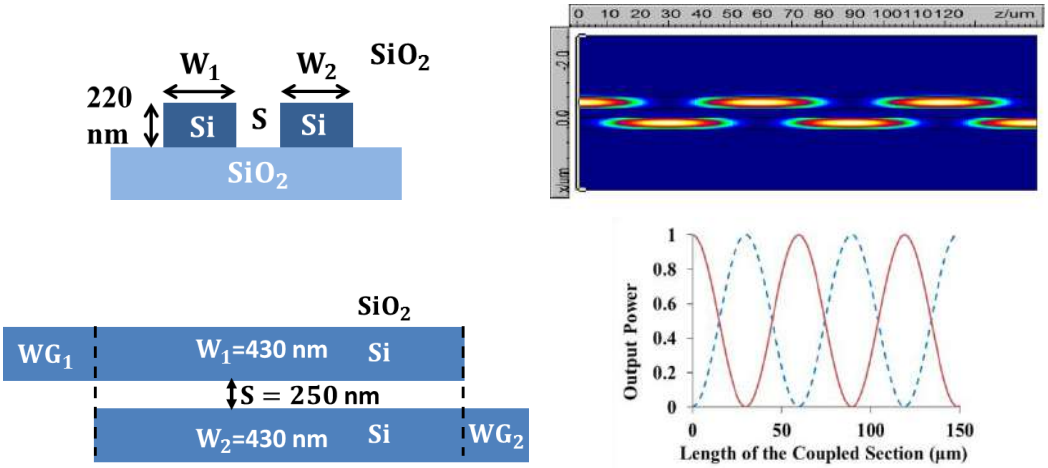

Fig 4. Cross-section and top view of a directional coupler formed with two identical silicon strip waveguides. The intensity profile of the propagating field through the coupled waveguides when power is launched shows a complete exchange of power; the line plots show the variation of power in WG_1 (red cont) and WG_2 (blue dashed) with propagation length.

A similar set of simulations for a directional coupler with two non-identical waveguides is shown in Fig 5. The silicon strip waveguides are assumed to be of different widths. As predicted by the coupled mode analysis there is still a periodic exchange of power between the waveguides but only a small fraction of the complete power is transferred to the second waveguide at the coupling length. However, at two times the coupling length, power completely returns to the launching waveguide.

Synchronous waveguides in a directional coupler are not necessarily identical waveguides but waveguides which have the same propagation constants, i.e. $\Delta\beta = 0$. As an example, we take a look again at two waveguides of unequal widths as shown in Fig 5 in which the refractive index of the guiding strip in the narrow waveguide (WG_2) is increased to 3.5510 while for WG_1 it remains as 3.4757 to obtain synchronous waveguides at the wavelength of 1550 nm. Again, as predicted by the coupled mode analysis there is a periodic exchange of power between the waveguides with complete power transfer at the coupling length as shown in Fig 6. Refractive index in silicon can be tuned thermally or by carrier injection while in some electro-optic materials like Lithium Niobate by application of an electric field.

It was also noted in section 2 that when power is input into a coupler from one waveguide,WG_1, at twice the coupling length the power returns to WG_1 with an additional phase factor of π in the amplitude as compared to the case in which it would have traversed the same length in WG_1 itself. This is clearly seen in the numerical simulation results shown in Fig 7.

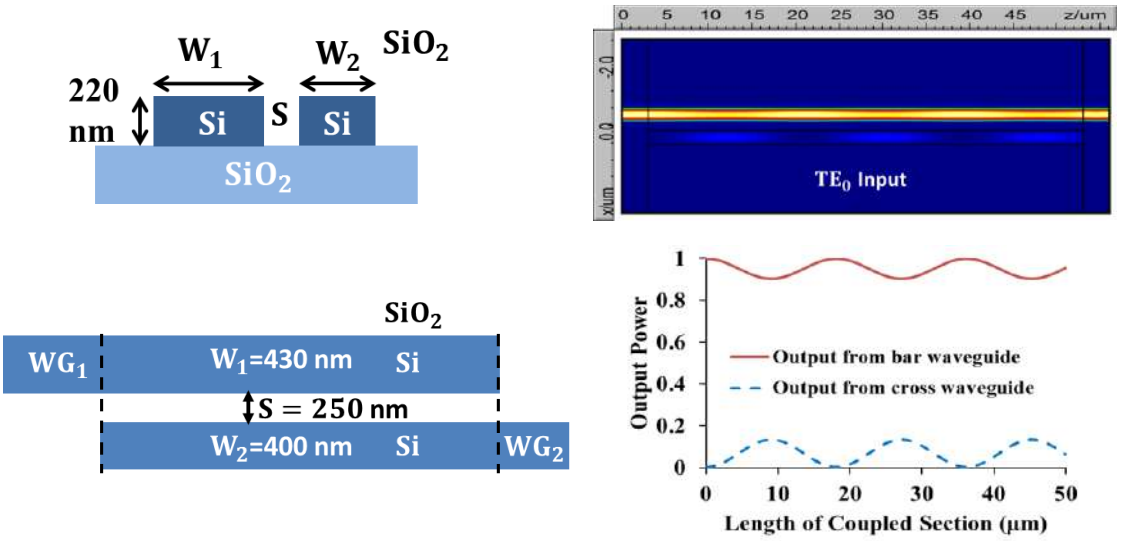

Fig 5. Cross-section and top view of a directional coupler with non-identical silicon strip waveguides. The intensity profile of the propagating field through the coupled waveguides when power is launched in WG_1 shows that only a small fraction of power is coupled; the line plots show the variation of power in WG_1 (red cont) and WG_2 (blue dashed) with propagation length.

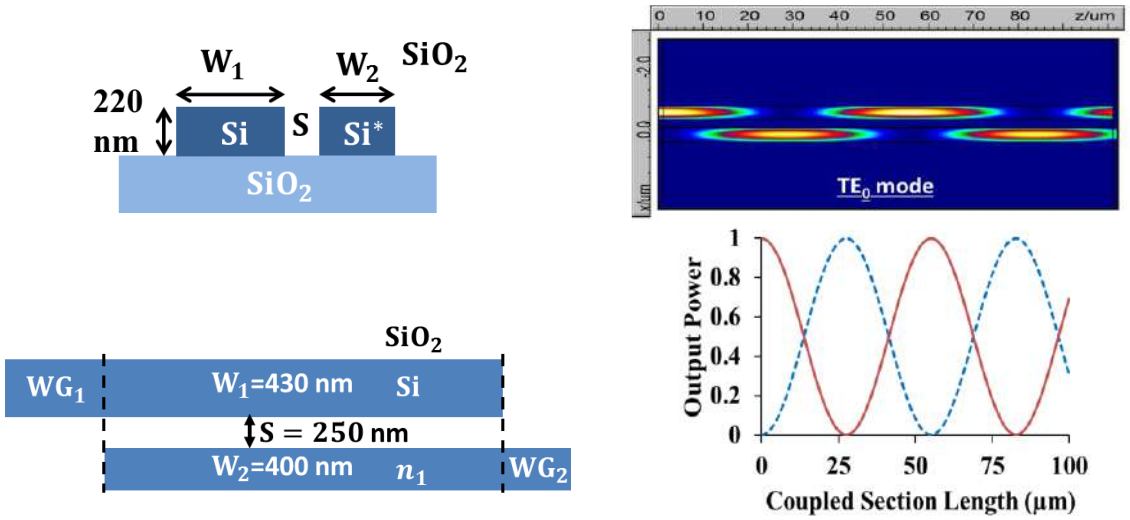

Fig 6. Cross-section and top view of a synchronous non-identical silicon strip waveguides directional coupler with index n_1 = 3.551 for phase matching. The intensity profile of the propagating field through the coupled waveguides when power is launched in WG_1 shows complete exchange of power; the line plots show the variation of power in WG_1 (red cont) and WG_2 (blue dashed) with propagation length.

The characteristics of the supermodes defined by coupled mode analysis can also be seen in the simulated results. The propagation constants or effective indices of the two supermodes vary with the waveguide spacing. An increase in waveguide spacing, S, essentially reduces the coupling coefficient, κ, and hence the effective indices of the two supermodes converge to the values corresponding to the individual waveguides. Figure 8 (a) and (b) shows the variation of effective index of the two supermodes with spacing for both identical and non-identical coupled waveguides geometries.

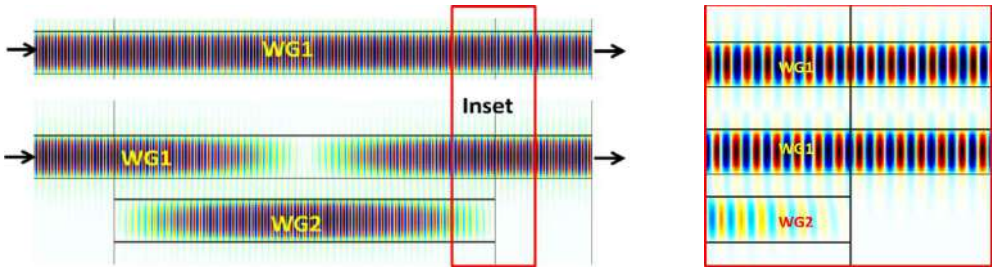

Fig 7. Power propagating through WG_1 and identical waveguide coupler with input from WG_1. Showing that at twice the coupling length the power returns to WG_1 with a phase difference of π in the amplitude. An expanded view of the inset shows the phase difference with clarity.

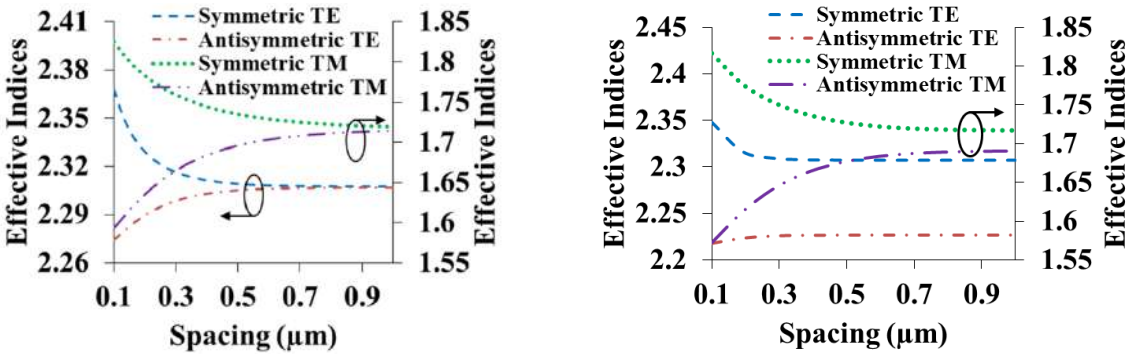

(a) (b)

Fig 8. Variation of the effective indices of the TE and TM supermodes with the waveguide spacing for (a) identical waveguides ($W_1 = W_2 = 430$ nm) coupler and (b) non-identical waveguides coupler ($W_1 = 430$ nm and $W_2 = 400$ nm) at 1550 nm wavelength.

The modal fields of the supermodes of the coupled waveguide configuration with identical waveguides are shown in Fig 9. As predicted by the coupled mode analysis, the mode profile of the symmetric and antisymmetric supermodes correspond to the sum and difference, respectively, of the mode profiles of the individual waveguide modes.

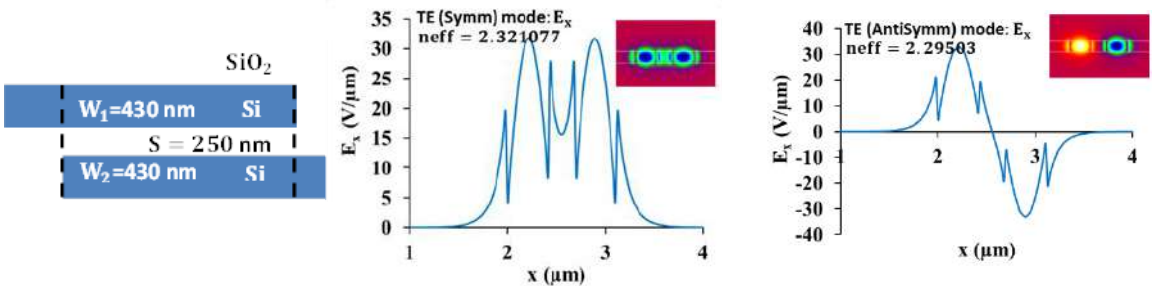

Fig 9. Modal fields of the symmetric and antisymmetric TE supermodes of the coupler with identical waveguides.

If the coupled waveguides configuration consists of non-identical waveguides with a large difference in the individual waveguide effective index ($\Delta n_{eff} = 0.178219$) as shown in Fig 10, the "symmetric supermode" and "anti-symmetric supermode" mode fields match the mode profiles of the wider and narrower waveguide, respectively.

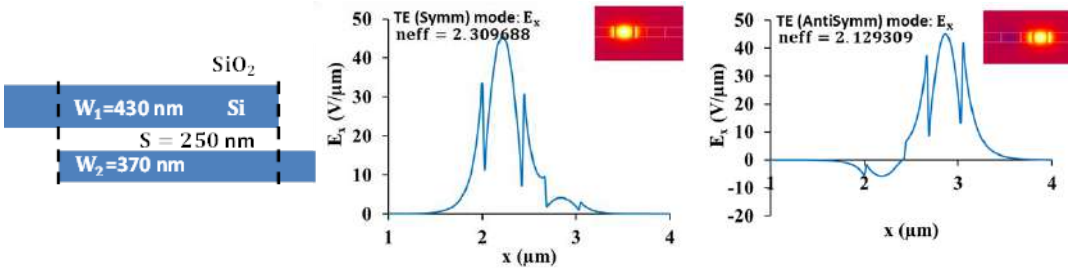

Fig 10. Modal fields of the symmetric and antisymmetric TE supermodes of a coupler with non-identical waveguides of different widths.

5 Coupled waveguide photonic devices

In this section, we present various coupled waveguide geometries which are essentially variants of the simple directional coupler and can be used for various applications like power dividers or splitters, switches, phase shifters, polarizers and mode division multiplexing.

5.1 Directional couplers for power dividing/splitting

The directional coupler in its simplest form can be used as a beam splitter or power divider by appropriate choice of the interaction length between the waveguides. Figure 11 shows typical directional couplers of varying interaction lengths and hence, coupling ratios formed with identical SOI waveguides of the type shown in Fig 4 with spacing S = 250 nm. The effective indices of the symmetric and antisymmetric supermodes are obtained as 2.32107 and 2.29503, respectively giving a coupling length of 29.75 µm. As predicted by the coupled mode analysis an interaction length of half the coupling length, $L_c/2$, gives a 3dB coupler with power equally divided in the two arms, for an interaction length equal to the coupling length power is completely transferred to the second waveguides and at twice the coupling length, power completely returns to the launching waveguide. The interaction lengths need to be corrected by ~ 5 µm to take into account the coupling, which occurs in the arms of the S-bend required for isolating the two waveguides.

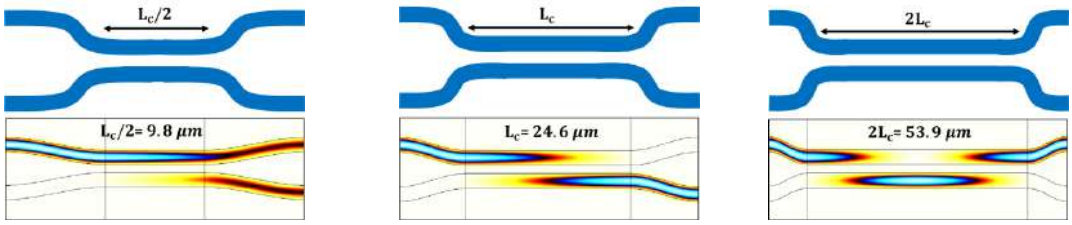

Fig 11. Typical identical waveguides directional coupler configurations with varying interaction lengths: $L_c/2$ for a 3dB coupler, L_c for complete transfer of power to the coupled waveguide and $2L_c$ for power to return to launching waveguide.

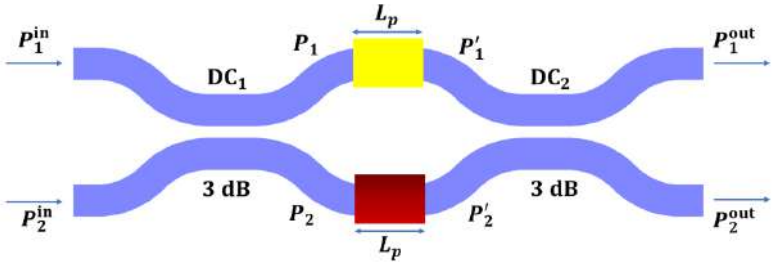

Fig 12. Typical Mach Zehnder configuration with 3dB couplers for power division in the two arms of the phase shifter section.

A 3dB directional coupler forms an important component of a typical Mach-Zehnder Interferometer (MZI) in integrated optics. For switching applications, the conventional MZI configuration shown in Fig 12 utilizes two 3dB couplers separated by a phase shifter section, with active control in either one arm or in both arms to form a switch.

If the phase accumulated by the two arms in the phase shifter section are equal or an integral multiple of 2π, the whole structure, the input and output directional coupler along with the phase shifter section will behave as a single directional coupler with interaction length equal to the coupling length and the input power gets transferred to the other coupled waveguide resulting in a cross-state. On the other hand, if the phase accumulation difference between the two arms of the phase shifter section is an odd multiple of π, the power is obtained at the output from the same waveguide resulting in a bar state.

5. 2 Coupled waveguide switch based on phase change material

Optical phase change materials (O-PCMs), which can be reversibly transitioned between the amorphous and crystalline phase by slow/fast heating, have recently emerged for various photonic applications. O-PCMs exhibit a very large difference in both the real part (greater than a factor of 1.5) and the imaginary part (at least an order of magnitude) of the refractive index between the two states. A high differential loss between the states of an O-PCM like $Ge_2Sb_2Te_5$ (GST) can be used to realize an optical ON-OFF switch in SOI waveguides. To achieve this Dhingra *et al* [11] have proposed a coupled waveguide configuration of the type shown in Fig 13, where the mode of the primary 500 nm wide silicon waveguide ((WG_1) can be coupled to the mode of the waveguide formed by ITO-GST-ITO stack (WG_2) through appropriate phase matching. The bottom and top ITO layers can also act as the electrodes for the application of required voltage to change the state of GST via Joule heating. For GST, the complex refractive indices at 1550 nm are given as 7.45+ j1.49 and 4.6+ j0.12 for the crystalline and amorphous state, respectively and 1.9595+ j0.0023 for ITO. The coupled waveguides are phase matched for GST in the crystalline state and the length L is chosen as the corresponding coupling length to ensure that power is completely out-coupled from the silicon waveguide. For GST in the low loss amorphous state, the corresponding $\Delta\beta$ is large and no power is out-coupled from the primary silicon waveguide. Hence, in a device length of only 2.5 μm, a high extinction ratio of 36dB and a low ON-state insertion loss of 0.72dB are obtained.

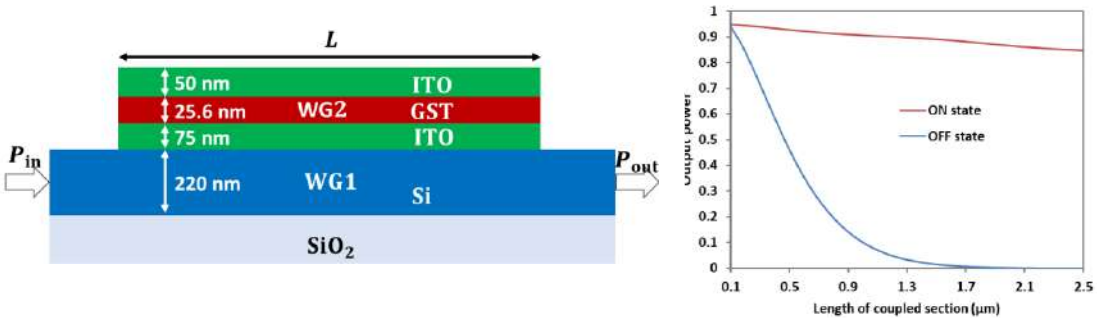

Fig 13. Side view of the proposed ON-OFF switch on a 500 nm wide silicon waveguide evanescently coupled to the ITO-GST-ITO overlay waveguide and its performance characteristics.

5. 3 Coupled waveguide phase shifter based on phase change material

Recently Dhingra *et al* [12] have proposed a design of a compact phase shifter based on an O-PCM for use in one arm of a conventional MZI configuration on the silicon nitride (refractive index: 1.9793) platform, shown in Fig 14, for 2 × 2 switching with low insertion loss and crosstalk. The chosen OPCM, $Ge_2Sb_2Se_4Te_1$ (GSST), offers a low loss in the telecommunication band in comparison to GST in both amorphous and crystalline state. The complex refractive indices of GSST at wavelength 1.55 μm are taken

as 5.074 – *j*0.425 and 3.413 – *j*0.00018 in its crystalline and amorphous phase, respectively. The design of the phase shifter is based on evanescent coupling between a silicon nitride waveguide and silica-GSST-silica waveguide as shown in Fig 15 similar to the design of the ON-OFF switch discussed in Section 5.2. However, in this design, the waveguides are phase matched with the O-PCM waveguide in its amorphous state to allow coupling where the waveguides are highly phase mismatched in the crystalline state to avoid interaction.

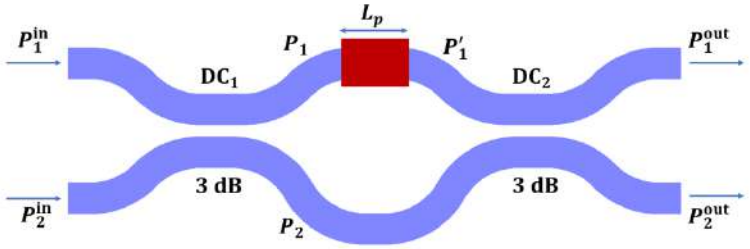

Fig 14. The conventional MZI configuration with typical silicon nitride on silica strip waveguides of dimensions 400 nm × 600 nm with active phase control on one arm to create a 2×2 switch.

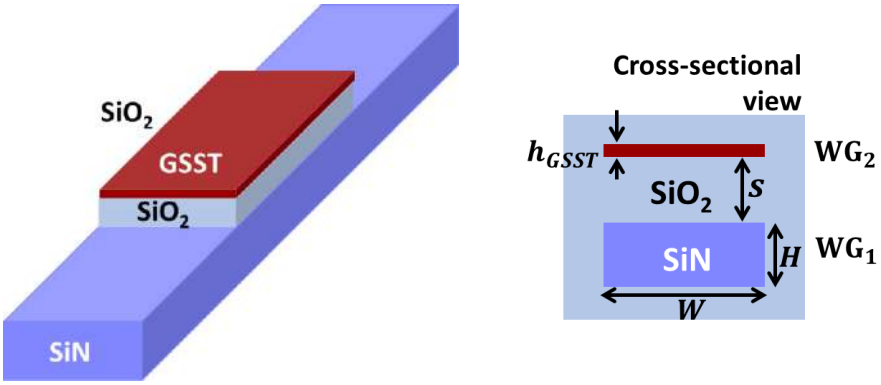

Fig 15. The phase shifter section for active phase control with a silicon nitride waveguide of dimensions 400 nm×600 nm coupled with GSST overlay of 58 nm separated by a silica buffer of thickness 600 nm for active phase control on one arm of the MZI to create a 2×2 switch.

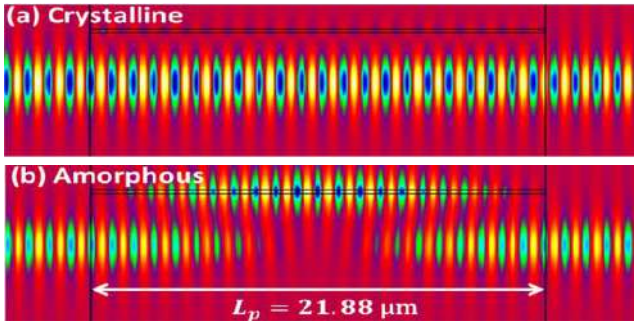

Fig 16. Field (H_y) through the coupled waveguide phase shifter section for GSST in (a) crystalline state and (b) amorphous state. The phase difference of π can be seen between the propagating field after coupling back at twice the coupling length in the phase matched coupler (b) and propagating straight through in (a).

As predicted by coupled mode theory, the power launched in accumulates an additional phase of π after propagating through an interaction length equal to twice the coupling length with the O-PCM in amorphous state in comparison to the propagation through the same length in WG_1. This leads to a phase difference of π between the two arms in the amorphous state for a phase shifter length of only ~ 21.88 μm, whereas no interaction in the highly lossy crystalline state ensures no phase difference and low insertion loss. Figure 16 clearly shows the difference in the accumulated phase in the two states. Hence, for GSST in crystalline state, the switch will be in the cross state for either input whereas for GSST in its amorphous state will give a bar state.

5. 4 Coupled waveguide based TE-pass polarizer

Metal-clad waveguide polarizers are perhaps the most studied with either the metal layer directly deposited on the cover or separated by a high index or low index buffer layer. However, the design of such polarizers has been usually based on parametric simulations. Now with an understanding of surface plasmon modes supported by a metal dielectric waveguides, these polarizers can be understood in terms of coupling between the guided TM mode of the dielectric waveguide and the lossy surface plasmon TM mode of a dielectric-metal-dielectric (DMD) waveguide [13]. Figure 17 shows a TE-pass polarizer designed for SOI waveguides based on evanescent coupling between the SOI dielectric waveguide and a specifically designed DMD waveguide for phase matching between the guided TM mode of the dielectric waveguide and surface plasmon TM mode supported by the DMD waveguide [14]. The single moded silica-silicon-silica waveguide with width 500 nm and thickness 210 nm supports one TE and TM mode with n_e (*TE*) = 2.4074 and n_e (*TM*) =1.7038 at 1.55 μm. With the metal layer directly deposited on the silica cover the effective index of the TM mode supported by the DMD waveguide SiO_2 –Au–Air is much lower than that of the silicon waveguide. To increase this value for phase matching a higher index buffer of silicon nitride (Si_3N_4) with optimized thickness needs to be added as shown in Fig 17 and the phase matched plasmonic ridge waveguide is now the SiO_2 –Si_3 N_4 – Au–Air waveguide.

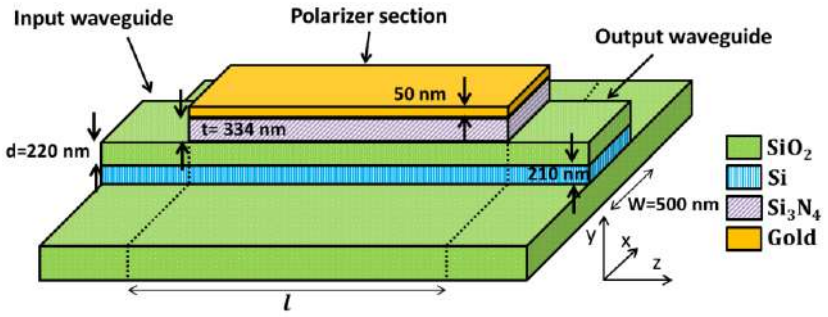

Fig 17. TE-pass polarizer for SOI waveguides. The TM mode of the input waveguide is completely attenuated by coupling to the phase matched lossy TM mode of the SiO_2 – Si_3 N_4 –Au–Air plasmonic waveguide.

The finally designed TE–pass polarizer section supports one TE mode with n_e (TE) = 2.4094 which is the same as that of the silicon input waveguide and two TM supermodes with effective indices, n_{es} (TM_0) = 1.8296 – *j*0.014 and n_{ea} (TM_1) = 1.6746 – *j*0.014. The TE mode is not coupled out and is transmitted without any change through the polarizing section. The TE mode is not coupled out and is transmitted without any change through the polarizing section. The TM mode is periodically coupled to the lossy TM mode of the plasmonic waveguide and hence by appropriate choice of the length *l* can be completely suppressed. The simulated performance of the polarizer is shown in Fig 18. The TE mode is transmitted without any change through the polarizing section while the TM mode is periodically coupled to the lossy TM mode of the plasmonic waveguide and hence in a short length *l* ~ 5 μm can be completely suppressed.

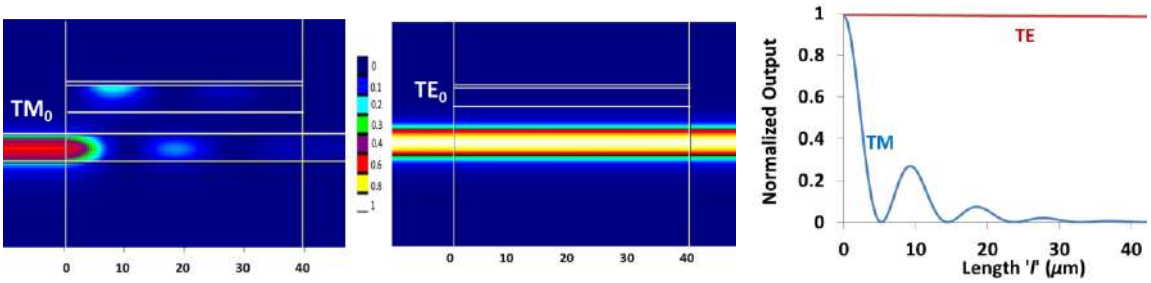

Fig 18. Simulated performance of the TE-pass polarizer for SOI waveguides. The TM mode of the input waveguide is completely attenuated by coupling to the phase matched lossy TM mode of the SiO_2 – Si_3N_4 –Au–Air plasmonic waveguide in a polarizer section of length ~ 5 μm while the TE mode is transmitted without change.

5. 5 Mode division multiplexers in optical interconnects

As also mentioned in section 3, if one of the waveguides (WG_2) supports more than one mode and the effective indices of the modes are well spaced, it is possible to couple power by evanescent coupling to any one of the modes. This can be done by choosing the single mode waveguides (WG_1) to be phase matched to a specific mode of WG_2. Figure 19 shows the effective index of various TE modes supported by the strip waveguide as a function of the strip width. A multimode waveguide (WG_2) with strip width of 900 nm supports three TE modes with effective indices n_e (TE_0) = 2.72166, n_e (TE_1) = 2.31472 and n_e (TE_2) = 1.605359. The fundamental mode (TE_0) of the input single mode waveguides with strip width of 433 nm and 252 nm are phase matched (i.e. with same effective index) to TE_1 mode and TE_2 mode of WG_2, respectively, as shown in the Fig 19. Hence, it is possible to couple/out-couple power between these single mode waveguides and the specific phase matched mode of the multimode waveguide. The simulated results, clearly showing coupling to a specific mode, are shown in Fig 20.

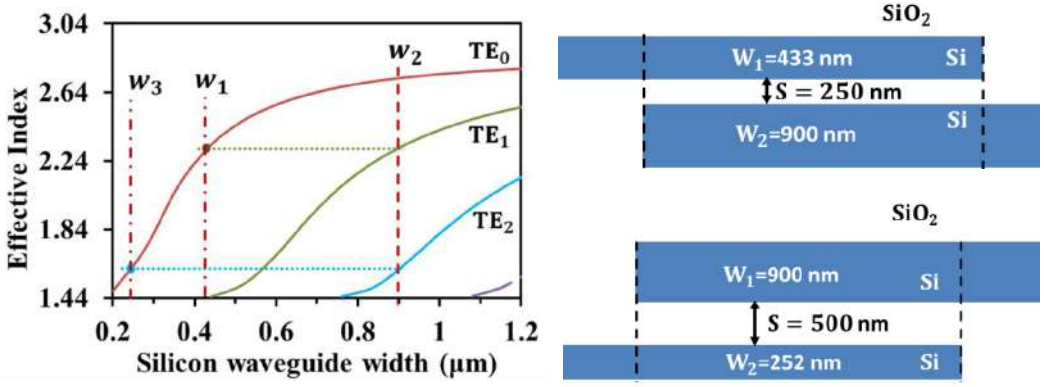

Fig 19. Variation of the effective index of possible guided TE modes as a function of strip width in a 220 nm thick SOI strip waveguide. The corresponding asymmetric directional couplers for evanescent coupling to different modes by choice of the appropriate width of the single mode input waveguide for phase matching are also shown.

This concept of coupling from different input waveguides to different modes of a multimode waveguide can be used to design compact add-drop multiplexers for mode division multiplexing in multimode SOI waveguide for on-chip and inter-chip optical interconnects [15,16]. Mode Division Multiplexing (MDM) offers increased bandwidth on a multi-mode trunk waveguide by use of different guided modes to carry different data channels coupled through different single-mode waveguides. Two independent channels can be coupled/decoupled from/to two collaterally arranged single-mode SOI waveguides (WG_1 and WG_3) to a multimode SOI trunk waveguide (WG_2) as shown in Fig 20.

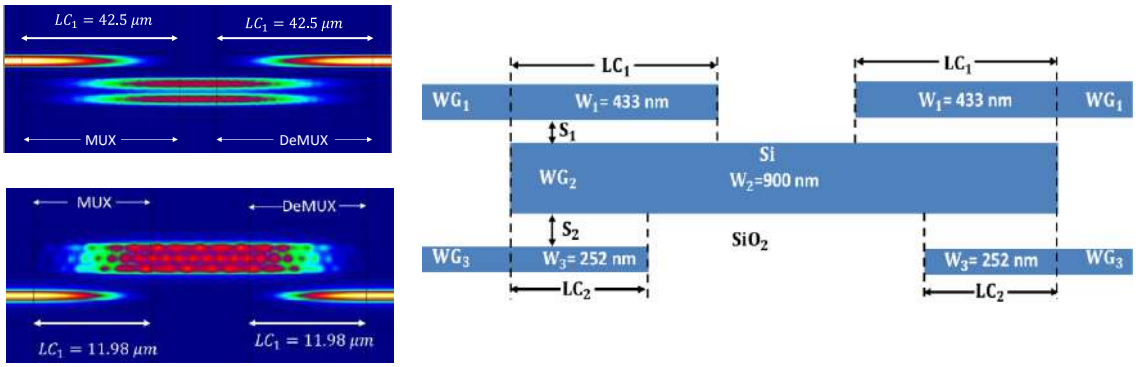

Fig 20. Propagation of power from TE_0 mode of WG_1 to TE_1 mode of WG_2 and subsequent out-coupling to WG_1 and propagation of power from TE_0 mode of WG_3 to TE_2 mode of WG_2 and subsequent out-coupling to WG_3. Configuration for mode division multiplexing by coupling two independent channels from collaterally placed single-mode SOI waveguides (WG_1 and WG_3) to a multimode SOI trunk waveguide (WG_2).

Figure 21 shows the design of proposed mode division (de)multiplexer based on this concept in which a simultaneous insertion/extraction of power carried by the TE_0 mode of WG_1 and WG_3 can be achieved to/from the selected modes of the trunk waveguide while the power in the TE_0 mode of the trunk waveguide is inserted/extracted through adiabatically tapered section connecting it to a 500 nm waveguide [15]. The total coupling length of the proposed (de)multiplexer section is ~ 24 μm and the complete device exhibits low insertion loss less than 0.26dB and crosstalk better than –36dB at the design wavelength of 1550 nm. The number of mode channels can be further increased by increasing the number of collateral coupler section along the trunk waveguide [16].

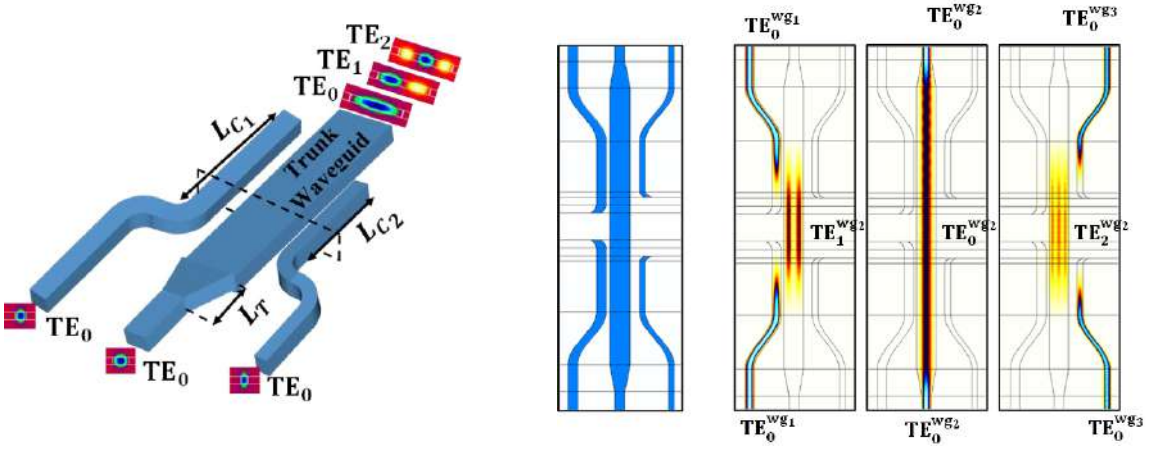

Fig 21. Prospective view of the proposed mode (de)multiplexer for three-mode multiplexing and simulated results showing the propagation of the modes through the trunk waveguide coupled/decoupled by evanescent coupling through phase matched mode single mode input waveguides at 1550 nm.

6 Summary

In summary, we have presented a detailed analysis of coupled mode theory for evanescent field coupling between modes of two dielectric waveguides placed close to each other in context to the most versatile coupled mode device, a two-waveguide directional coupler. The salient features emerging from the analysis have been illustrated by comprehensive numerical simulations using the Photon Design software

which is based on the Finite Element Method and Eigen-Mode expansion techniques. The dielectric waveguides chosen for our illustrative examples are the Silicon-on-Insulator (SOI) waveguides which form the backbone of the silicon photonics integrated circuits. It has been a fascinating journey for us across two decades to realize how the simple variants of the directional coupler can be used to design a number of guided wave photonic devices. We have presented a few such coupled waveguide device configurations for applications as power dividers, switches, phase shifters, polarizers, and mode division multiplexers.

Acknowledgements

The first author (EKS) would like to acknowledge all her Ph D students who have contributed to the understanding of coupled modes in fibres waveguides and design of novel coupled mode photonic devices across a long journey of almost four decades.

References

1. Huang W P, Coupled-mode theory for optical waveguides: an overview, *J Opt Soc Am A*, 11(1994)963-983.
2. Hardy A, W. Streifer W, Coupled Mode Theory for Parallel Waveguides, *J Light Technol*, 3(1985)1135-1146.
3. Syms R R A, Improved coupled-mode theory for codirectionally and contradirectionally coupled waveguide arrays, *J Opt Soc Am A*, 8(1991)1062-1069.
4. Vassallo C, About Coupled-Mode Theories for Dielectric Waveguides, *J Light Technol*, 6(1988)294-303.
5. Haus H A, Huang W, Coupled-mode theory, *Proc IEEE*, 79(1991)1505-1518.
6. FIMMWAVE/FIMMPROP, Photon Design Ltd, http://www.photond.com
7. Gupta N, Sharma E K, Modified variational analysis of coupled waveguides, *J Opt Soc Am A*, 10(1993)1549-1552.
8. Kohli N, Srivastava S, Sharma E K, Scalar coupled mode theory and variational analysis for planar SOI waveguide arrays: a detailed comparison, *Opt Quant Electron*, 48(2016)265; doi.org/10.1007/s11082-016-0540-z.
9. Kohli N, Srivastava S, Sharma E K, Orthogonal solutions for asymmetric strongly coupled waveguide arrays: an elegant, analytical approach , *J Opt Soc Am B*, 31(2014)2871-2878.
10. Rumpf R C, Coupled Mode Theory, 21st Century Electromagnetics, Available: https://www.youtube.com/watch?v=pZ_alesCCPo.
11. Dhingra N, Song J, Ghosh S, Zhou L, Rahman B M A, Design of phase change $Ge_2Sb_2Te_5$ based on-off electro-optic switch, Silicon Photonics XIII, International Society for Optics and Photonics., vol. 10537, p. 105370Z, Feb. 2018.
12. Dhingra N, Song J, Saxena G J, Sharma E K, Rahman B M A, Design of a Compact Low-Loss Phase Shifter Based on Optical Phase Change Material, *IEEE Photon Technol Lett*, 31(2019)1757-1760.
13. Sital S, Sharma E K, Design Methodology for metal clad polarizer in SOI waveguides, International workshop on Optical Wave and Waveguide Theory and Numerical Modelling (OWTNM)-2015, City University London, UK, 16-18 Apr. 2015.
14. Sital S, Sharma E K, Design Menthology for TE-Pass Polarizer in SOI waveguides, *Opt Quant Electron*, 48(2016) 369; doi. 10.1007/s11082-016-0636-5.
15. Nath J P, Dhingra N, Saxena G J, Sharma E K, Compact Mode Division Multiplexed On-Chip Interconnect based on Evanescently Coupled SOI Waveguides, The International Conference on Fiber Optics and Photonics, Indian Institute of Technology Delhi, India, 12-15 Dec. 2018.
16. Nath J P, Dhingra N, Saxena G J, Sharma E K, Compact Mode Division (de)Multiplexer Based on Collaterally Coupled SOI Waveguides, *IEEE Photon Technol Lett*, 32(2020)595-598.

[*Received*: 12.03.2021; *accepted*: 26.04.2021]

Nikhil Dhingra received the B.Sc. degree in physics and the M.Sc. degree in electronics from the University of Delhi, India, in 2011 and 2014, respectively. He is currently pursuing the Ph D degree in the area of photonics from the Department of Electronic Science, University of Delhi, India, with his research interest in the design and analysis of coupled mode photonic devices. He has been the recipient of Junior Research Fellowship (JRF) by the UGC, New Dehli, India. He has been a visiting fellow at City University, London with the INTACT fellowship under ERASMUS MUNDUS programme by European Union and is a recipient of the Shastri Research Student Fellowship (SRSF) by Shastri Indo-Canadian Institute for collaborative research with University of Ottawa, Canada.

Jyoti Prasad Nath received the B Sc degree in electronics from the Dibrugarh University and the M Sc degree in electronics from the Guwahati University, India, in 2014 and 2016, respectively. He is currently pursuing the Ph D degree in the area of photonics from the Department of Electronic Science, University of Delhi, India, with research interest in the design of guided wave photonic devices and special interest in mode division multiplexing devices. He is the recipient of INSPIRE fellowship by Department of Science and Technology (DST), Government of India.

Enakshi Khular Sharma is a retired Professor from Department of Electronic Science, University of Delhi South Campus. She received the B Sc degree from Meerut University, India, in 1973, the M Sc Degree in Physics and Ph D degree from Indian Institute of Technology Delhi, India in 1975 and 1979, respectively. She continued to work at the Indian Institute of Technology Delhi till July 1985. In July 1985 she joined University of Delhi South Campus as a Reader in the Department of Electronic Science where where she has been a Professor since 1995. Her research interests are in the area of photonic devices with emphasis on analysis, design and simulation of optical fibre and waveguide devices and more recently in the area of optical control of passive microwave devices on semiconductor substrates and bio-sensors. Her work has resulted in more than 100 publications in Journals and International and National Conferences. She has supervised over 20 Ph D theses and a number of M Sc, M Phil and M Tech dissertations. Her work has also been supported by sponsored research grants from MIT, DRDO, UGC and University of Delhi. She has had collaborations with Jean Monnet University, France, University of Karlsruhe, Germany, University of Sheffield, City University London and Kyushu University, Japan as a partner in the Indo-Japan Collaboration Project (2006-2009) on “Infrastructural Communication Technologies Supporting Fully Ubiquitous Information Society”. Apart from that, she has also served many other positions at the University of Delhi including as the Head, Department of Electronic Science, Director, Centre for Canadian Studies, etc. She is a member of IEEE, Optical Society of America, SPIE and fellow of the Optical Society of India.